JMEPEG (2011) 20:1128–1139
DOI: 10.1007/s11665-010-9759-1

1059-9495/$19.00

Neural and Neural Gray-Box Modeling for Entry Temperature Prediction in a Hot Strip Mill

José Angel Barrios, Miguel Torres-Alvarado, Alberto Cavazos, and Luis Leduc

(Submitted September 28, 2009; in revised form June 15, 2010)

In hot strip mills, initial controller set points have to be calculated before the steel bar enters the mill. Calculations rely on the good knowledge of rolling variables. Measurements are available only after the bar has entered the mill, and therefore they have to be estimated. Estimation of process variables, particularly that of temperature, is of crucial importance for the bar front section to fulfill quality requirements, and the same must be performed in the shortest possible time to preserve heat. Currently, temperature estimation is performed by physical modeling; however, it is highly affected by measurement uncertainties, variations in the incoming bar conditions, and final product changes. In order to overcome these problems, artificial intelligence techniques such as artificial neural networks and fuzzy logic have been proposed. In this article, neural network-based systems, including neural-based Gray-Box models, are applied to estimate scale breaker entry temperature, given its importance, and their performance is compared to that of the physical model used in plant. Several neural systems and several neural-based Gray-Box models are designed and tested with real data. Taking advantage of the flexibility of neural networks for input incorporation, several factors which are believed to have influence on the process are also tested. The systems proposed in this study were proven to have better performance indexes and hence better prediction capabilities than the physical models currently used in plant.

Keywords Gray-Box modeling, hot rolling, hot strip mills, hybrid modeling, neural networks, semiphysical modeling, temperature estimation

1. Introduction

A hot strip mill (HSM) transforms steel slabs or ingots forms obtained by continuous or traditional casting into coiled strips. A typical hot rolling line consists of the following stages: furnaces or soaking pits, roughing mills (RMs)—sometimes one or two reversible RMs, finishing mill (FM), cooling banks, and down coilers. Figure 1 shows the hot rolling line where this study was undertaken. When the study was carried out, the mill was equipped with soaking pits, numbered from 1 to 22 in Fig. 1. Currently, this HSM is working with a walking beam furnace, and less dispersion on temperature would be expected. A final strip coil of a HSM must attain required thickness, width, and mechanical properties (Ref 1).

After the slab leaves the furnace, at about 1300 °C, it is transported for roughing, in this case two reversible RMs, see Fig. 1. Here, the initial thickness reduction takes place usually with 5 or 7 passes. The next stage is the FM which often consists of 6 or 7 stands; Fig. 2 shows a schematic of a FM stand. When it is in the FM, the bar is called strip. At the FM exit, the strip has to fulfill final thickness, width, and finishing temperature specifications, the last one is required to achieve the desired mechanical properties. When the strip leaves the FM, it is taken to the cooling banks where the strip has to be cooled down from the finishing temperature to a specific coiling temperature which is also required for mechanical properties.

The most critical process stage in hot rolling is the FM. It involves a great number of variables due to the interaction between stands and requires a higher level of automation (Ref 2). The initial set points for FM controllers; for both, thickness and finishing temperature control; have to be calculated before the incoming bar enters the mill for the bar front section (bar head-end) to meet requirements. In order for the initial set points to be calculated, some rolling variables, particularly temperature, at bar head-end have to be estimated. Such estimation must be performed on-line and in the shortest possible time to preserve heat (Ref 2). Thus, temperature estimation at the bar head-end is a major concern in hot rolling, and it is performed from measurements at the exit of the RM since the bar surface is more clean at this point (Ref 1, 2) and it is not affected by recalescence (Ref 3). The set of values of the calculated variables required for the FM to work is usually called "mill set up."

Currently, in most mills, rolling temperature estimation is performed by physical modeling (Ref 2). This is carried out in cascade from the RM exit temperature, as mentioned above, according to the different thermal phenomena involved (Ref 2). Figure 1 shows in blocks this cascade estimation process. First, estimation at the FM entry descaler, usually called secondary scale breaker (SB), is performed; the FM entry descaler can be seen in Fig. 1 labeled with letter D. The output of this model is fed to the models that calculate the temperature at the SB exit. Then this estimation is used to predict the rolling temperature within the roll gaps in the FM for each stand, see Fig. 2. The

José Angel Barrios, Miguel Torres-Alvarado, and **Alberto Cavazos**, Universidad Autónoma de Nuevo León, Av. Universidad S/N, Cd. Universitaria, Apdo. Postal 115, C.P. 66450 San Nicolás de los Garza, NL, Mexico; and **Luis Leduc**, Ternium Mexico, Av. Los Ángeles 325, San Nicolás de los Garza, NL, Mexico. Contact e-mails: acavazos@fime.uanl.mx and alberto.cavazosgz@uanl.edu.com.

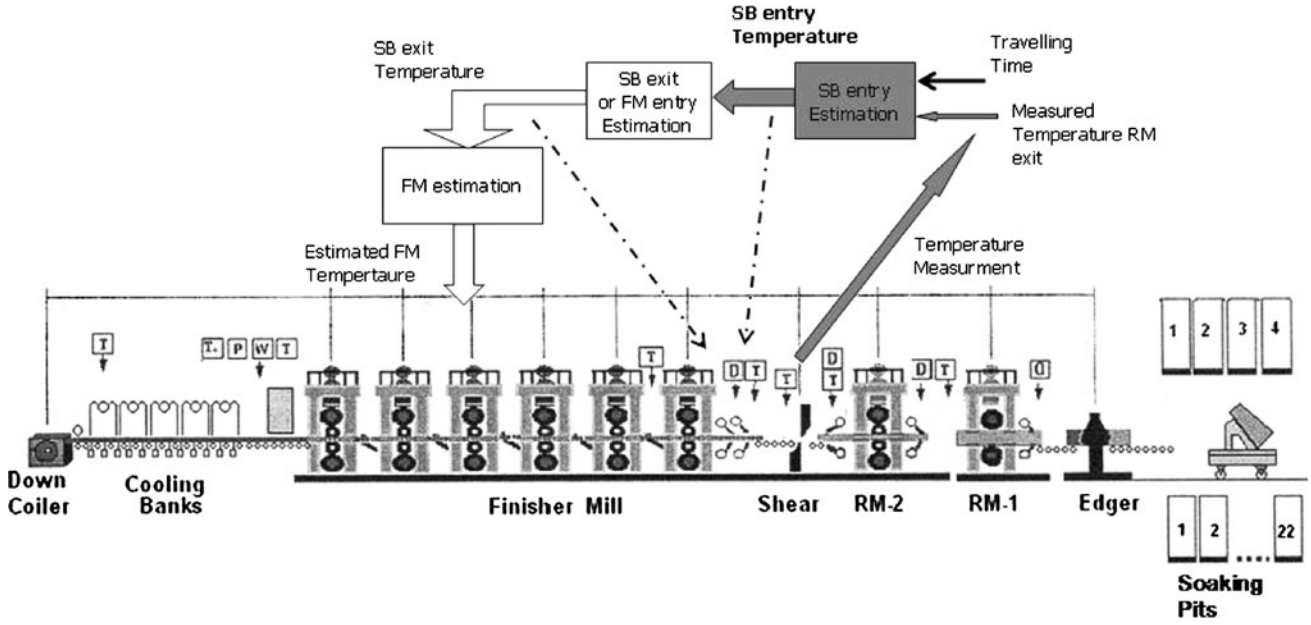

Fig. 1 Hot rolling mill production line with temperature prediction block diagram

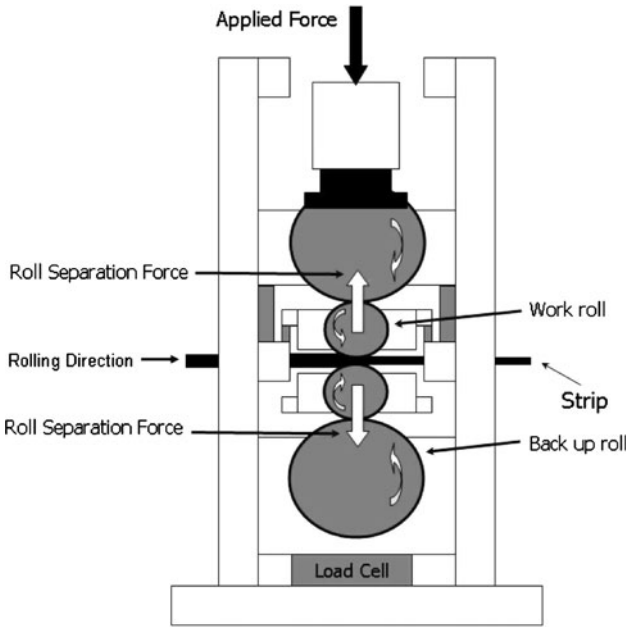

Fig. 2 Schematic diagram of a hot strip mill stand

dashed lines in Fig. 1 indicate the corresponding points to the estimated temperatures. Nonetheless, only the FM estimated temperature is used for set point calculations. This study is concerned with the bar head-end temperature estimation at the entry of the SB, first block (shadowed) in Fig. 1 (Ref 1, 2).

Usually, the physical modeling estimation error is compensated by an additive proportional plus integral (PI) structure as shown in Fig. 3, which will be described in detail later (Ref 2). It can be noticed from Fig. 3, that the PI structure is compensating the current prediction with previous bar prediction error assuming that current conditions are similar to the former ones. Therefore, measurement uncertainties, variations in the process, and continuous product changes may have detrimental effects on estimation, i.e., large estimation error and therefore a faulty mill set-up, leading to a non-conformational bar head-end (Ref 4), and thereby reducing process efficiency.

However, in order to overcome the aforementioned problems, estimation systems based on Artificial Intelligence (AI) techniques, such as Artificial Neuronal Networks (ANNs) and Fuzzy Logic (FL) have been proposed. Such artificial intelligent technologies offer the advantage of estimating nonlinear function without having complete knowledge of the process as well as adaptation and learning (Ref 4-6). Adaptation and learning confer the ANN the prediction capabilities under a diversity of operating conditions.

A Gray-Box system basically consists of two systems of different nature. The first is usually a physical model based on a phenomenological representation of the process, and the second system is based on a different technique namely AI. Therefore, the already mentioned advantage of the ANN also applies for neural-based Gray-Box modeling. In Ref 7, it is mentioned that Gray-Box models are prediction models with greater accuracy and a wider range of conditions. On the other hand, FL is a powerful technique to model nonlinear relations incorporating empirical knowledge. The combination of these techniques, i.e., neuro-fuzzy systems, captures the advantages of both technologies.

Another advantage of the ANNs over the physical model as implemented by finite differences is that the time consumed for computing is less. In addition, the ANNs are simpler to adapt and use since it only requires minimal training, allowing a better approximation.

There are two other merits of Gray-Box models. Gray-Box models allow taking advantage of the equipment already installed in plant since it introduces an additive term to the physical model used to set-up the mill; hence, the commissioning stage is much faster and safer. The great disadvantage of AI techniques is the lack of physical interpretation that is something very much desirable from process engineering and trouble-shooting stand point; nonetheless, this is overcome by Gray-Box modeling since it contains a physical model within its structure.

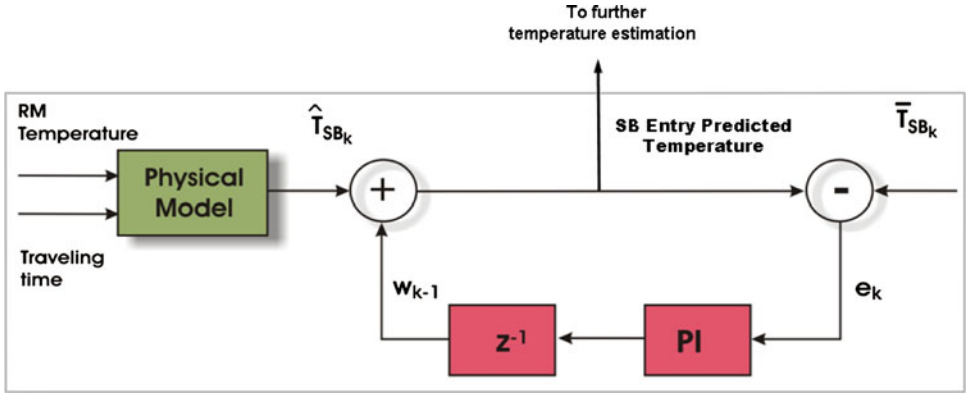

Fig. 3 Physical model with a PI compensation structure

In the forthcoming paragraphs, a literature review showing the success of AI techniques in a HSM is presented; these techniques have proven, given their adaptation and learning capabilities, to be suitable for processes involving highly varying operating conditions as well as measurements' uncertainties. First, the FL applications are shown, followed by ANN and neuro-fuzzy works. Gray-Box modeling is also reviewed beginning with industrial applications in general, followed by applications specific to hot rolling.

One of the early studies carried out in this field is presented in Ref 8. A Fuzzy Inference System (FIS) was developed to compensate the thickness error based on the physical model force prediction error in two intermediate stands in the FM. A system which integrates the operator expertise and a FIS to set-up gaps and speeds in the FM is presented by Watanabe et al. (Ref 5). Several ANN-based systems for the estimation of FM variables, such as force, stack temperature, and full set-up have been proposed (Ref 4, 6, 9-12).

Mendez et al. (Ref 13) have proposed bar head-end entry temperature prediction of a HSM using a hybrid learning neural-fuzzy type-2 FIS. Min-You (Ref 14) has proposed material property prediction using neural-fuzzy networks. Mahfouf et al. (Ref 15) presents the use of neural-fuzzy techniques for modeling and optimization of the mechanical properties of alloy steels in heat treatment and hot rolling.

One approach proposed in the literature for the estimation of the variables is the so-called Gray-Box Methodologies (also called Hybrid or Semiphysical Models). As mentioned, a Gray-Box model basically consists of systems of two different types. The first is usually a physical model based on a phenomenological representation of the process, wherein the physical model used in plant will be considered. The second system is based on a different technique, that is, AI, Gray-Box modeling will be described in Section 5. In Ref 7, a review of Gray-Box modeling and its industrial applications is presented, justifying its use for meeting the great demand that exists in the prediction models for material production with greater accuracy and a wider range of conditions.

In the industry in general mainly ANN-based Gray-Box modeling has been used for variable estimation, for example, in a waste water plant (Ref 16), for synthesis in liquid process phase of the methanol (Ref 17), for modeling the sucrose crystal growth rate (Ref 18), and the retention process in papermaking (Ref 19). An application of a neuro-fuzzy-based Gray-Box model can be found in Ref 20.

Applications of ANN-based Gray-Box models have also been found in the steel industry: see Hodgson et al. (Ref 21) for prediction of the hot strength in steels and Schlang et al. (Ref 22) who present the current and future development of neural computation including neural-based Gray-Box models.

Geerdes developed one parallel and two series connection structures of Gray-Box models for temperature prediction in a HSM. It is demonstrated that the use of Gray-Box systems have potential advantages with respect to ANN or a physical model alone (Ref 23).

1.1 Objectives and Scopes

As can be seen from the previous section, ANNs and neural-based Gray-Box models have not been fully explored for temperature estimation in a HSM. The ultimate goal is to improve head-end temperature estimation; however, the first purpose of this study is to explore and evaluate the applications of neural techniques, ANN, and neural Gray-Box models, for bar head-end SB entry temperature estimation, given the relevance of this variable in the calculation of initial controller set points, and hence in final strip quality fulfillment. Several ANNs and neural-based Gray-Box models have been designed and tested. Their performances are compared to those of the physical model with PI compensation used in plant as depicted in Fig. 3 using five performance measures (PMs). The main reason for the Gray-Box models to be studied in this work is that they have the advantages of keeping a model based on the physical knowledge which is important for process engineering and that they allow a safer commissioning stage.

Another advantage of the ANNs is that they allow the incorporation of new inputs without significant changes on the ANNs architecture or a deep knowledge of the process; while incorporation of new entry in physical modeling requires a great amount of effort. This capability allowed testing several factors which are believed to be important for SB entry temperature estimation but not considered by the physical model, this being a second purpose of this work. Thus, ANNs and neural-based Gray-Box systems incorporating additional entries for such factors were also developed and tested.

The physical model used currently in plant to estimate temperature is used here as a benchmark, a detailed description of which is out of the scope of this study, it being a very well-established theory (Ref 3, 24); in Section 3, however, it is briefly described.

Neural Networks theory details are also out of the scope of this study; the fundamentals are briefly described; for details see Ref 25.

2. Description of the Problem

Figure 2 shows a schematic representation of a mill housing of a FM stand. The inner rolls in contact with the strip are called work rolls, and the outer and larger rolls are called backup rolls. The actuator used to supply the vertical force for bar deformation is frequently a hydraulic cylinder. The vertical force is directly acting on the back up rolls.

Every FM stand has to achieve a particular proportion of thickness reduction accurately. In order to have a more stable rolling process, a specific strip tension between the slabs is needed, which is supplied by devices called loopers. Tension also contributes to thickness reduction. Therefore, thickness, finishing temperature, and tension, among other variables, should be controlled when the strip is being rolled within the FM. However, the controllers set points are not straightforwardly obtained since the incoming bar conditions, such as temperature and resistance, may vary from bar to bar. Final product specifications may also change. Therefore, the initial set points for controllers have to be calculated and sent to controllers before the incoming bar enters the FM; otherwise head-end may not conform to the required specifications.

2.1 Initial Set-Points Calculations

The exit thickness at intermediate stands is calculated, among other variables, from initial and final thicknesses. Suppose a stand i has to attain an exit thickness h_i for given initial and final thicknesses. When a specific strip is being rolled, the reaction force, called roll separation force, will produce deformation of the stand housing since it is not infinitely stiff, see Fig. 2. This will cause the gap between rolls to widen. This deformation is called stretch. Therefore, the reference of the cylinder position regulator should be set such that the gap between rolls equals h_i minus *stretch*. Thus, the stretch has to be known to calculate the cylinder position regulator set point before the bar enters the mill; otherwise, the strip head-end may not fulfill quality specifications. Stretch depends on the force required for bar thickness reduction; in plant, an experimental stretch/force curve is periodically obtained. Notwithstanding, since force measurements are available only after the bar is in the FM, force has to be predicted, which depends on bar resistance which, in turn, depends on steel grade and bar temperature. Thus, the calculation of the initial cylinder position regulator reference requires that the incoming bar head-end entry temperature be known beforehand.

On the other hand, in order to achieve the specified finishing temperature at the bar head-end, since the mill cannot add heat, a specific strip speed is required. Mill speed would depend on the difference between the bar entry temperature and the required finishing temperature. This involves a number of calculations of heat loss and gain at each stand since temperature is not measured at every stand for economic and physical reasons. However, calculation of the initial reference of the motor drivers requires as well the knowledge of the incoming bar head-end entry temperature before the bar enters the mill.

2.2 Problem and Proposed Solution

From the above discussion, it can be concluded that rolling temperature at bar head-end, among other variables, have to be known before the bar enters the FM to calculate both, the initial hydraulic cylinder position (which determines thickness) and the motor speed (used for controlling the finishing temperature). Since conditions along the bar change, after the bar has entered the mill, initial set points are adjusted by the automatic gauge control and the finishing temperature control. The more accurate the temperature predictions are the faster the controllers converge; hence, temperature prediction (among other variables) is of crucial importance for both, the bar head-end and the bar main body to fulfill quality requirements.

However, temperature measurement at FM entry is not reliable because of oxide formation (Ref 1, 2) and recalescence (Ref 3); consequently, it has to be estimated from RM exit measurements which are more reliable. As can be seen in Fig. 1, RM exit is equipped with a descaler device labeled with letter D. In Fig. 1, the temperature measurement points are labeled with the letter T; in this particular mill, the temperature that is used for temperature estimation is the one measured after the crop shear.

However, as mentioned above, measurement uncertainties, variations in the process, and continuous product changes may have detrimental effects on estimation, i.e., large estimation error and therefore a faulty mill set-up, leading to a non-conformational bar head-end (Ref 4). In order to overcome the aforementioned problems, estimation systems based on AI techniques such as ANNs and FL have been proposed.

This study is concerned with the bar head-end temperature estimation at the SB entry by ANNs and neural Gray-Box models, given its importance for both, bar head-end and bar body to meet requirements.

3. Temperature Model Description

In this section, the physical model used currently in plant is briefly described; the details are out of the scope of this study, since the model is used here only as benchmark for comparison purposes. The reader should consult Ref 3, 24 for a deeper insight on temperature physical modeling. Figure 4 shows a flow chart of the SB entry temperature estimation sequence.

As can be seen in Fig. 4, in practice, traveling time is also calculated. Every 5 s, the bar is checked for arrival to SB entry area, if bar has not arrived yet, the temperature calculation is performed adding 5 s to traveling time; this will lead to a maximum traveling time error of 5 s. It should also be pointed out, that the PI calculation term is performed after the bar has arrived, and real SB temperature and traveling time have been measured. This is done in order for the PI term to compensate only for model temperature prediction errors with no influence of time miscalculations. It can also be noticed from Fig. 4 that the PI term to compensate current bar prediction error is calculated from the previous bar error.

Temperature modeling is performed by a one-dimensional (1D) finite difference algorithm, and it is based on heat conduction Fourier's first law and heat loss of the surface by radiation. The heat flow from and into one bar element is given by (Ref 3):

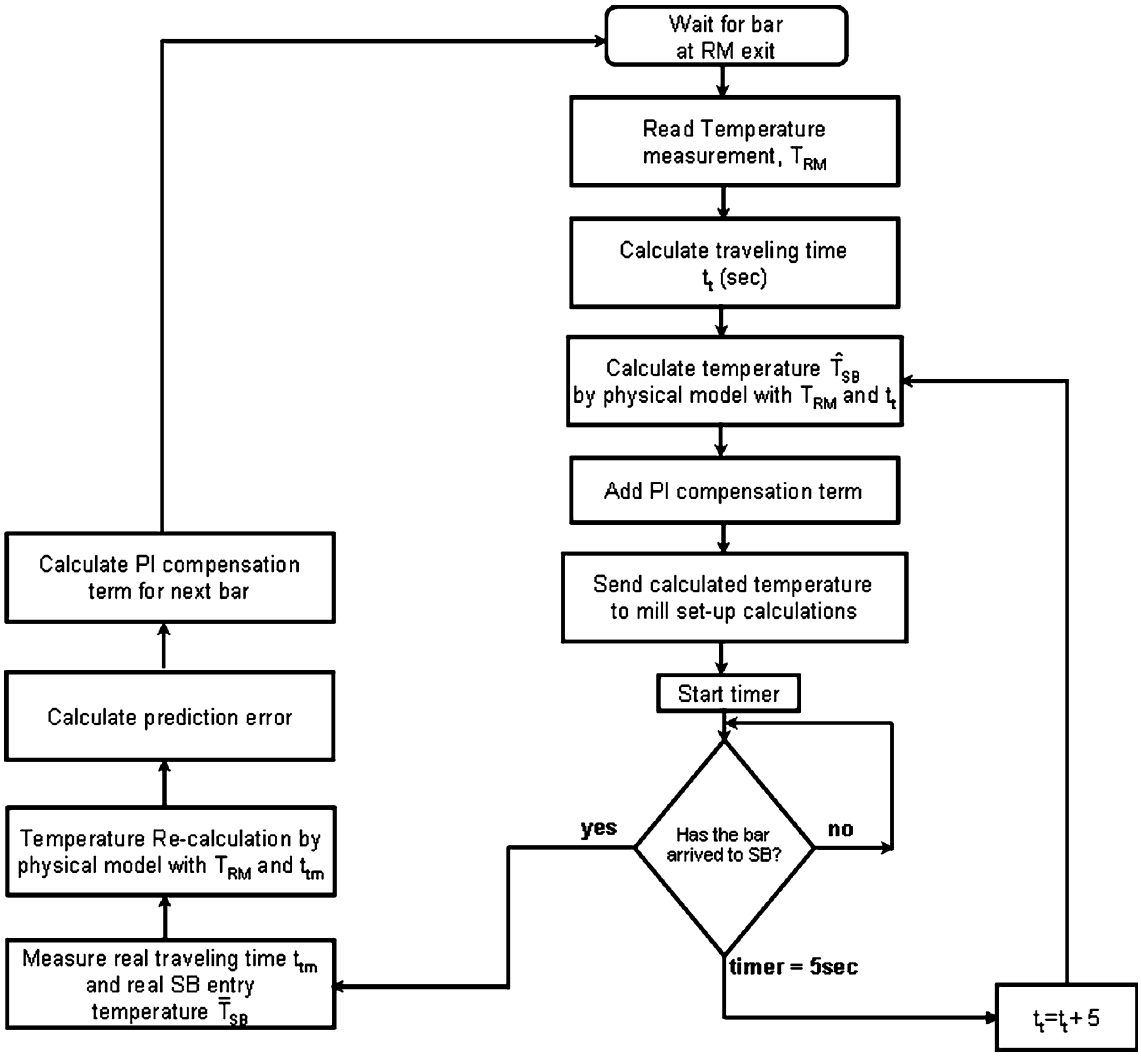

Fig. 4 Flowchart of SB entry temperature estimation process

$$Q_c = (T_1 - T_2)\frac{KA\delta t}{D} \quad \text{(Eq 1)}$$

where A is the area of the heat conducting path, D is the distant between elements, K is the thermal conductivity, and δt is the elapsed time.

Heat loss at the surface by radiation can be calculated as (Ref 3):

$$Q_r = (T_s^4 - T_A^4)\sigma A\varepsilon\delta t \quad \text{(Eq 2)}$$

where T_s is the surface temperature, T_A is the ambient temperature, σ is the Stephen-Boltzmann coefficient, and ε is the emissivity. Heat loss at surface and the thermal conductivity were experimentally tuned.

Heat loss through the oxide film is also considered, assuming the oxide layer as having zero heat capacity. The oxide heat loss is given by (Ref 24):

$$Q_o = (T_s - T_o)\frac{K_o}{D_o} \quad \text{(Eq 3)}$$

where T_o is the oxide surface temperature, K_o is the oxide thermal conductivity, and D_o is the oxide layer thickness.

The model calculates the bar surface and center temperatures at the SB entry from: (1) the surface temperature measured at RM exit at the end of the last pass after the shear (see Fig. 1), and (2) the traveling time from the RM exit (at the shear) to the SB entry, see Fig. 4. In this study, only the surface temperature at the bar head-end is to be estimated by the ANNs and neural Gray-Box models.

3.1 Physical Model with Proportional + Integral Additive Compensation

In general, mathematical models used to represent physical processes are approximations due to simplifications and neglecting of terms; leading to prediction errors. In some applications, these errors may be sufficiently small; however, in other cases, they have to be reduced. Such is the case of physical modeling that is used to predict temperature at the SB entry. In a number of HSM sites, the SB entry temperature physical model prediction error is reduced with an additive term calculated by a Proportional + Integral structure. The model prediction error is calculated and then a compensation is added to the next bar model temperature prediction, such scheme is referred in this study as model + PI and it is shown

in Fig. 3. In Fig. 3, k denotes the current bar while $k-1$ denotes the previous one; $\hat{T}_{SBk}$ and $\bar{T}_{SBk}$ stand for current model predicted and current measured SB entry temperatures, respectively, e_k is the current bar prediction error, and w_{k-1} is the PI compensation calculated from previous bar error. Figure 4 depicts a flowchart showing the prediction sequence including the PI compensation. As mentioned above, the PI compensation term is calculated from previous bar estimation error.

Estimations of the ANNs and neural Gray-Box models developed here are compared to those of the model + PI used in plant.

4. Neural Networks Fundamentals

In this section, a brief description of ANNs' fundamentals is presented; for a deeper insight, see Ref 25.

The particular ANN architecture used in this study is shown in Fig. 5. This feedforward ANN has layers of neurons with m, n, and r neurons in the input, hidden, and output layers, respectively. The neurons in the input layer receive the user's inputs and pass this information to the neurons in the hidden layer through arcs where certain weights modify the information in transit. The hidden neurons apply a transformation—commonly a nonlinear one—to the received weighted information and then pass the new data to the neurons in the output layer through a different set of connecting arcs and their respective weights. The neurons in the output layer transform the data once again—usually in a linear fashion in this point—and provide the predictions of the ANN.

The mathematical expression of the ANN shown in Fig. 5 is, then:

$$\mathbf{y} = f_2(\mathbf{v} f_1(\mathbf{w}^t \mathbf{x} + \mathbf{b}) + \mathbf{c}) \quad \text{(Eq 4)}$$

where

$$f_1(a) = \frac{1 - e^{-a}}{1 + e^{-a}} \quad \text{(Eq 5)}$$

is called the activation function; $f_2(a) = a$; $\mathbf{x}$ is an $m \times 1$ vector with values of independent input variables as elements; $\mathbf{w}^t$ is a transposed matrix with dimensions $n \times m$ that keeps the weights on the arcs joining the input neurons with the hidden neurons; $\mathbf{v}$ is an $r \times n$ matrix that holds the weights on the arcs going from the hidden neurons to the output neurons; vectors $\mathbf{b}$ and $\mathbf{c}$ of dimensions $n \times 1$ and $r \times 1$, respectively, contain weights that act as biases; and $\mathbf{y}$ is an $r \times 1$ vector containing the values of the dependent output variables. It is worth mentioning that there may be more than one hidden layer, changing Eq 4 accordingly. In this study, only ANNs with one or two hidden layers were used.

A critical decision called for when using ANNs is to determine the number of hidden layers and neurons to provide an adequate fit without sacrificing the ANN's prediction capabilities. Although many methods have been suggested for this purpose, a common one involves trying different numbers of hidden layers and neurons so as to find a compromise between the network's learning and generalization performance.

The ANN has to pass through a learning stage called training. Therefore, in order for the ANN to be trained, input/output real measured data from the process have to be collected—the data set used for training is called "training

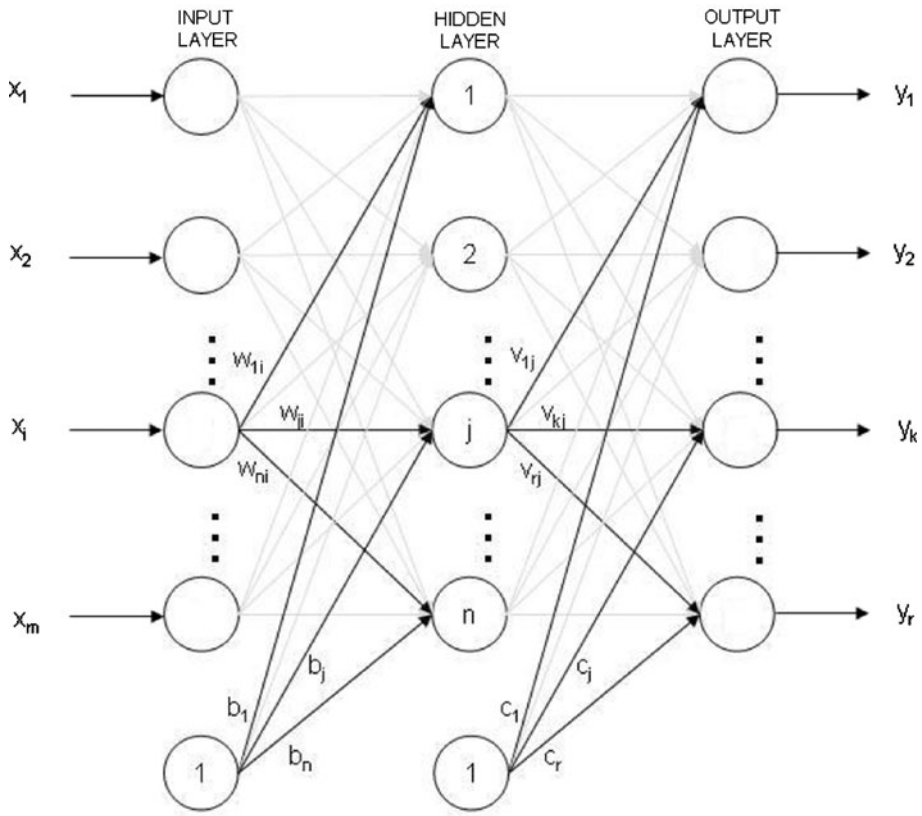

Fig. 5 Neural network architecture

data set." Every input/output record from the database is called "data pair." During training, the network's weights are optimized to minimize the prediction error measured typically with the mean squared error (MSE) over the training data set. The whole training data set is applied to the network a number of times until MSE is satisfactory: each time is called "epoch." Network's weight optimization is performed by the so-called "backpropagation" algorithm, in which the error is propagated backward from the output layer to the input one.

After training, the network's generalization capabilities have to be tested; then prediction has to be carried out over a different data set called "validation data set," however, from the same statistical universe as the training data set. The validation set is applied to the network only one epoch, usually with the weight adjustment disabled. A common practice is to randomly partition the database into two different sets one for training and one for validation.

4.1 Gray-Box Models

Gray-Box systems are those that combine a physical model with an AI system. The parallel Gray-Box is the most commonly found in the literature; it consists of two systems connected in parallel. In this study, the AI systems will be an ANN connected in parallel with the model + PI as shown in Fig. 6. As can be seen in Fig. 6, the ANN output is an additive term; hence, the ANN's prediction can be considered to be compensating an additive estimation error of the model + PI.

5. Methodology

In this study, the SB entry temperature is estimated by ANNs and neural-based Gray-Box models. The types of ANNs and neural-based Gray-Box models developed and tested here are feedforward ANNs with one or two hidden layers and 3, 5, or 7 neurons per hidden layer. The intention was to design lean ANNs to allow achieving faster convergence and short computation time.

The method described in Section 4 to train and validate the ANNs was used throughout this study. The ANNs were trained and tested; choosing the one with the best PMs over the validation data set. Performance evaluation of the developed systems is carried out by five PMs applied on the estimation error: the PMs are defined below.

The physical model used in plant predicts SB entry temperature from surface temperature measured at the exit of the RM, and the bar traveling time from the RM exit to the SB entry. These factors have been proven to influence the SB entry temperature prediction; hence, they were also chosen to be the inputs to the ANNs and Gray-Box models used in this study having the ANNs—two input neurons for x_1 and x_2 and only one neuron in charge of presenting the prediction for temperature (y).

As mentioned above, it can be seen in Fig. 4, that traveling time is calculated, having an error of 5 s at the most. Nevertheless, the measured traveling time is used to calculate the additive PI term to compensate only for the model estimation error. In this study, the measured traveling time will be used to evaluate the model + PI and the neural systems developed here. In this case, an estimation scheme as the one shown in the flowchart of Fig. 7 is assumed. Figure 8 depicts a flowchart showing the estimation scheme using a Gray-Box model.

One of the advantages of ANNs is that inputs can be incorporated without significant changes on ANNs architecture; also, a deep knowledge of the physical behavior of the process is not required at all. Some ANNs and ANN-based Gray-Box models were designed adding some extra inputs to test some factors not included in the physical model but considered to be important for the heat loss process. These factors are: steel composition in percent weight of carbon (x_3), manganese (x_4), silicon (x_5) and copper (x_6); RM previous pass screw position (x_7); RM previous pass force (x_8), and elapsed time between bars (x_9). Figure 9 shows the prediction flowchart corresponding to a Gray-Box model with additional factors.

Since in the Gray-Box model the ANN output is added to the model + PI estimation (see Fig. 6 and 8), the ANNs were designed to estimate the model + PI estimation error. Now the

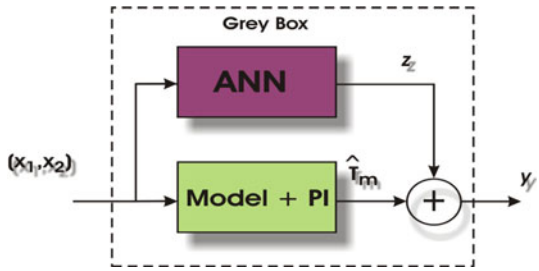

Fig. 6 Parallel Neural-based Gray-Box scheme

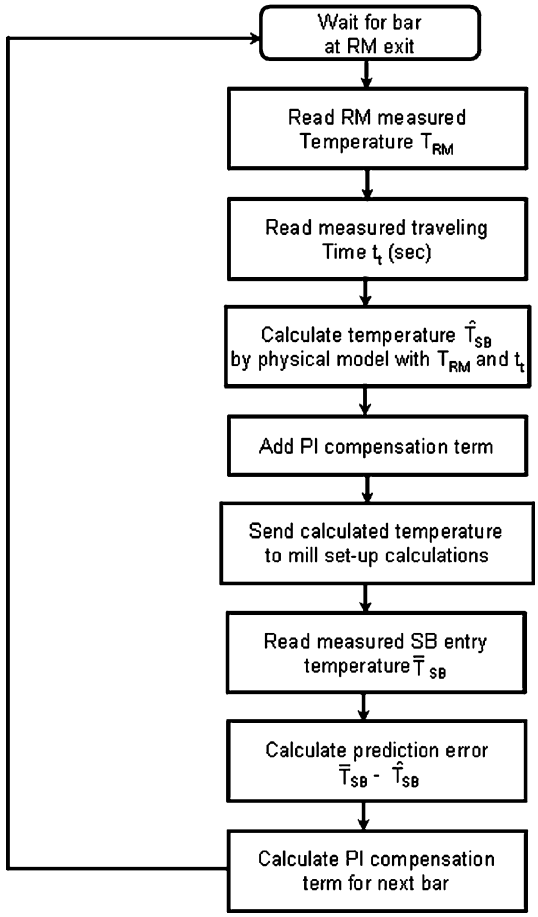

Fig. 7 Flowchart of SB entry temperature estimation process using measured traveling time

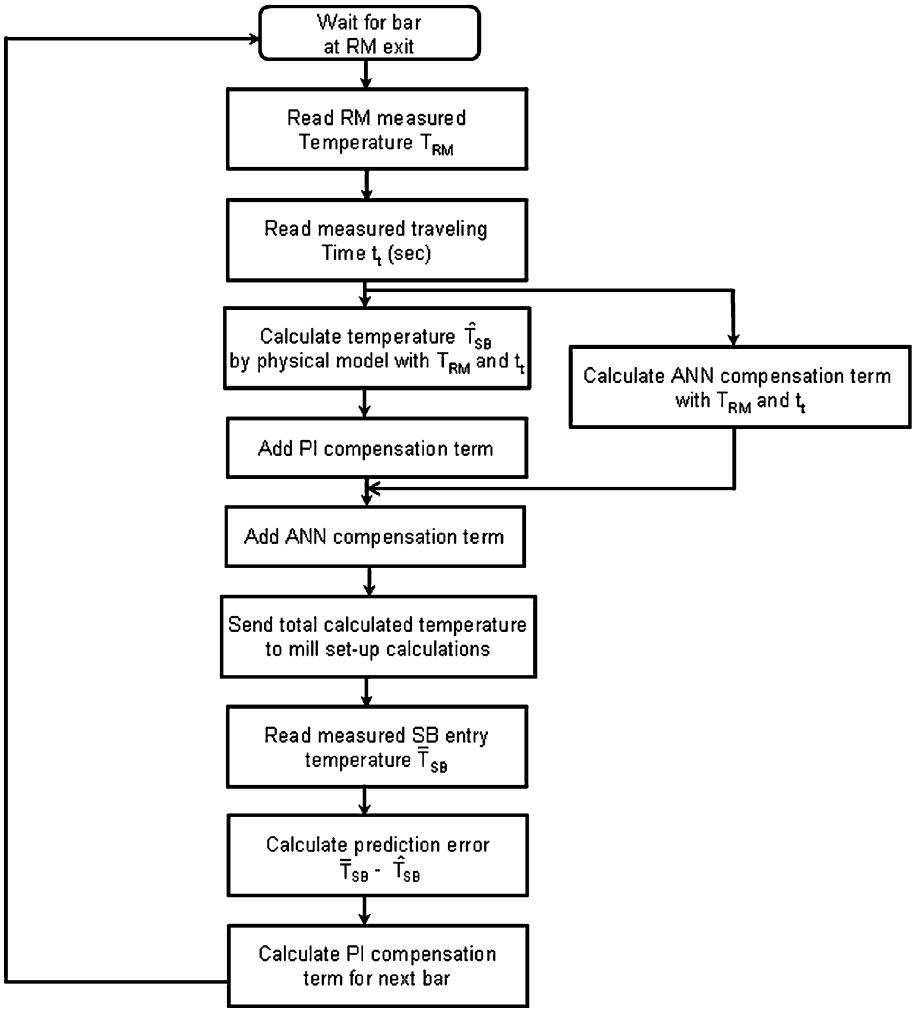

Fig. 8 Flowchart of SB entry temperature estimation process with Gray-Box model

ANN will have the same two inputs as the physical model (x_1 and x_2 as defined above) and one output, the ANN estimation of the model + PI estimation error (z). Note that the output of the Gray-Box model is still called y, while in Fig. 6, the model + PI estimation is called $\hat{T}_m$. The model + PI estimation error was calculated from the training data set. Their estimation error vector was used to train the ANNs. Once the ANNs systems were trained, the overall Gray-Box structures were built and evaluated using the validation set. Gray-Box systems to test the additional factors mentioned above were also designed, with the additional factors (x_3, x_4, x_5, x_6, x_7, x_8, and x_9) being these inputs only for the ANN and not for the model + PI in Fig. 6; see also Fig. 9.

All ANNs were developed using the software MATLAB™. The Levenberg-Marquardt algorithm is a variation of the traditional backpropagation learning algorithm which provides faster responses; for this reason, this algorithm was chosen in this study for training the ANNs.

As mentioned, five PMs were applied over system prediction errors with the validation set to evaluate the ANNs and Gray-Box models developed here. The estimation error is given by:

$$e = T_e - T_m$$

where T_e is the temperature estimated by the particular system to be evaluated, and T_m is the measured temperature both at SB entry area. The PMs are (1) mean error (ME): $\bar{e} = \sum_i e_i/N$, where N is the number of elements in the validation data set, and $i = 1, 2, 3,\ldots,N$ denotes the input/output data pair number; (2) standard deviation (SD): $\sigma_e = \sqrt{\sum_i (e_i - \bar{e})^2/N - 1}$; (3) mean absolute error (MAE): $|\bar{e}| = \sum_i |e_i|/N$; (4) root mean square error (RMSE): $e_{rmse} = \sqrt{\sum_i e_i^2/N}$; and (5) the percentage of bars of the validation data set with e_i within $\pm\Gamma$ °C, where Γ is a tolerance defined as follows.

A PM defining the percentage of bars within some specifications (#5 PM) would be very illustrative; however, in practice, there are no standard specification limits for entry temperature estimation error. Then, a reasonable number for Γ had to be chosen. According to one of the mill automation system manufacturers given as a "thumb rule," an estimation error of 14 °C will propagate into the FM and will create a 10% error force which may cause a 50-70-μm thickness error (Ref 2). Although this is only an empirical rule and no scientific proof is given, the manufacturer experience should not be neglected. It can be used as a reference number, and it would be desirable to choose a number not much greater than 14°. On the other hand, with the tolerance for finishing temperature control being ±20 °C, it is not preferable to exceed 20 °C. Therefore, for evaluation purposes only, in this

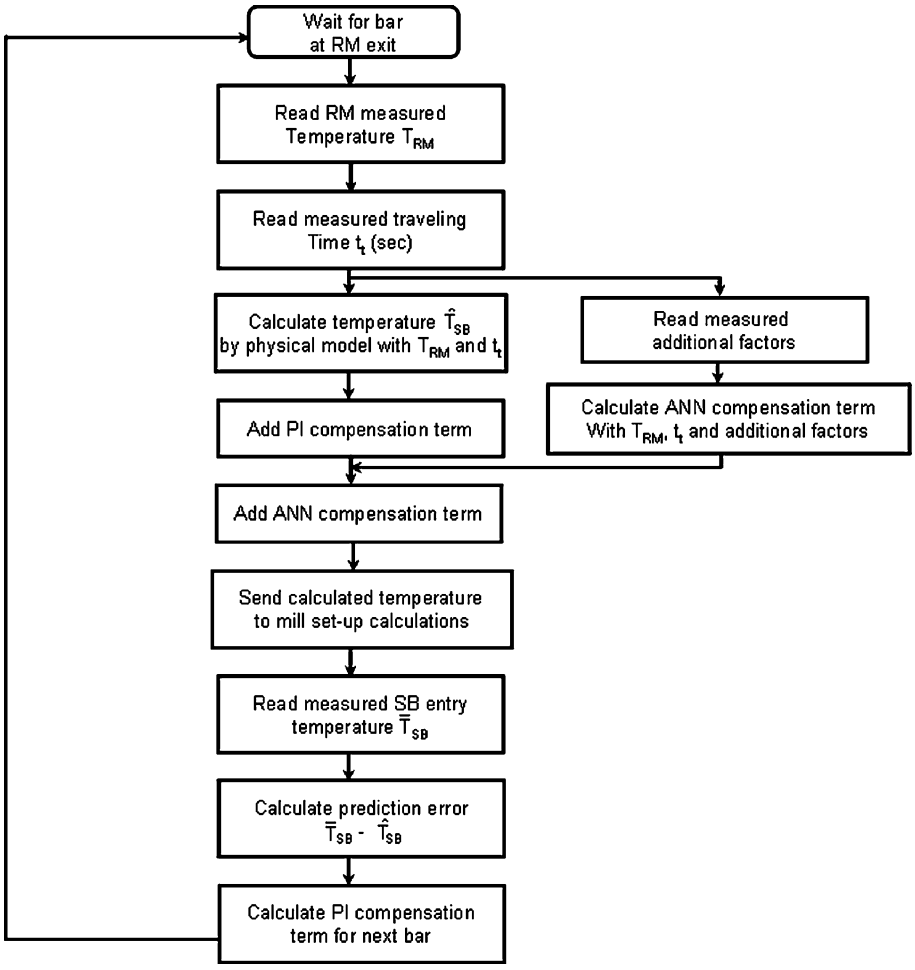

Fig. 9 Flowchart of SB entry temperature estimation process with Gray-Box model and additional factors

study Γ will equal 20. Thus, defining #5 PM as the percentage of bars with e_i within ±20 °C, is abbreviated as "% Bars within ±20 °C."

When evaluating the systems, a ME closer to zero is pursued while for SD, MAE, and RMSE, low values should be expected. A large percentage of bars with an estimation error within ±20 °C is desirable.

The study presented in Ref 23 is extended here by: (1) using a larger data set; (2) evaluating performance with two more indexes, i.e., RMSE and the percentage of bars within ±20 °C, this making the evaluation more conclusive; (3) testing factors other than those in the physical model; and (4) comparison against the model compensated by the PI structure as used in plant.

6. Results and Discussion

6.1 Experimental Data

The data used to carry out the experiments were collected from the HSM 1 of TERNIUM-Hylsa on-line and real-time basis; however, the system tests are run offline. Information of 748 bars of different degrees was collected, 60% of them was used for training, while the remaining 40% was used for validation. Figure 10 and 11 show dispersion diagrams of the

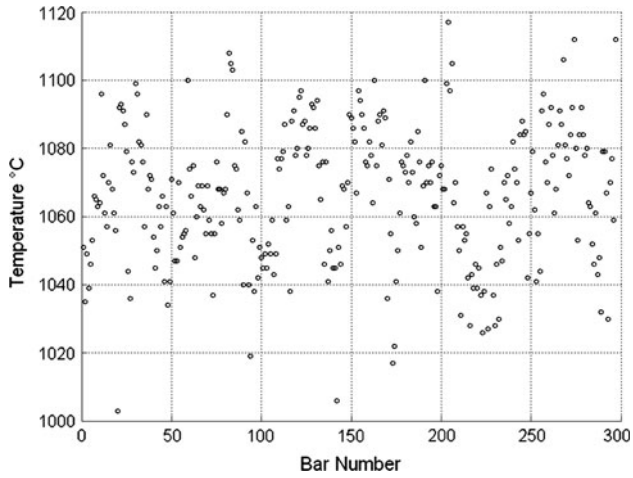

Fig. 10 Dispersion diagram of the RM exit measured temperature

measured RM exit temperature and measured SB entry temperature, respectively; Fig. 1 shows the temperature measurement points. It should be noted that, as pointed out, SB entry temperature measurement is not as reliable as that at the RM exit—thus, in practice, model + PI compensation is employed only after measurements have been checked and spurious measurements have been eliminated. However, in

general, in a noisy environment, as in the case of a hot rolling line, measurement errors may occur during data collection; therefore, all collected data were also checked before the systems were tested.

x_1 and x_2 ranges are [988-1124 °C] and [23-162 s], respectively, while the output variable y has a range of [810-1027 °C]. The input data were normalized between [−1 and 1] according to Eq 5.

6.2 Result Analysis

The ANNs developed as described in Section 5 were ANNs and ANN-based Gray-Box models with and without additional inputs. They have been tested after training for SB entry temperature estimation with the validation data set. As mentioned above, performance was evaluated using five different PMs applied on the estimation error. The model + PI was also tested, and its performance was evaluated for comparison purposes.

Table 1 shows the PMs of the best ANNs and Gray-Box models developed here, both with and without additional factors and that of the model + PI. The best results are highlighted in bold characters.

It can be noticed from Table 1 that ANNs and Gray-Box models PMs are very similar with Gray-Box models having only a slightly better performance to show than ANN in terms of "% Bars within ±20 °C" for the case when additional entries were not included. All the ANN and Gray-Boxes developed here have considerable better PMs than the model + PI. Therefore, they can be considered to have better prediction capabilities than the traditional system used in plant. This may contribute in practice to lower the number of non-conforming bars. This suggests that the neural systems are a feasible option for SB entry temperature predictions; however, in order to recommend their implementation in plant, some more exhaustive tests with larger data set should be performed.

It can also be seen in Table 1 that the incorporation of the additional factors brings ME much closer to zero than the systems without the additional entries, showing the latter as having larger skewness. Such additional factor produces an improvement of about 10% in terms of "% Bars within ±20 °C." Additional factors when incorporated to the ANNs improves performance showing their influence on the heat loss process, and the same deserves further study.

Figure 12 shows histograms of the model + PI, the ANN, and the Gray-Box. Only those neural systems without additional entries are shown to allow a better comparison with the model + PI. The results shown in Fig. 12 are consistent with those shown in Table 1; both neural systems have a mean value closer to zero and less dispersion than the model + PI, which yields a higher "% Bars within ±20 °C."

Figure 13 and 14 show dispersion diagrams of the model + PI and the Gray-Box-predicted SB entry temperatures versus measured SB entry temperatures, respectively. The 45° line indicates the ideal estimation. As can be observed in Fig. 13 and 14, Gray-Box prediction shows the less dispersion of both, this being consistent with results sown in Table 1 and Fig. 12; however, it can also be noticed that the best predictions are those at mid-temperatures; low- and high-temperature predictions have to be improved.

These results are promising, on the one hand, because of the advantage that the ANNs offer, i.e., less computing time required than that in the model implemented by finite difference. On the other hand, the Gray-Box model, which still works along with the finite difference model, is also improving prediction having the advantages of safer commissioning stage and a physical interpretation model.

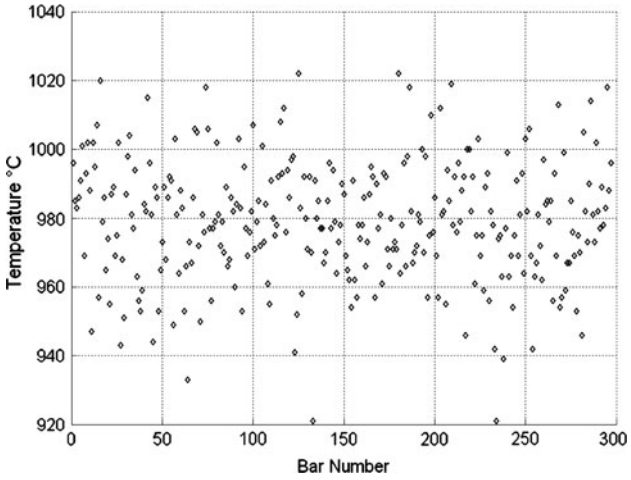

Fig. 11 Dispersion diagram of the SB entry measured temperature

Table 1 Performance indices for ANNs and Gray-Box models

System	SD	ME	MAE	RMSE	% Bars within ±20 °C
Without additional entries					
Gray-Box	15.9224	7.0843	14.0802	17.4679	75
ANN	16.1084	−8.2047	14.6147	18.0537	73
With additional entries					
Gray-Box	15.0723	−2.3862	**11.8331**	**15.2352**	**82.9**
ANN	**14.8299**	**−0.4108**	12.7222	16.0394	82
Model + PI	20.6479	−18.9096	23.3486	27.973	47.8

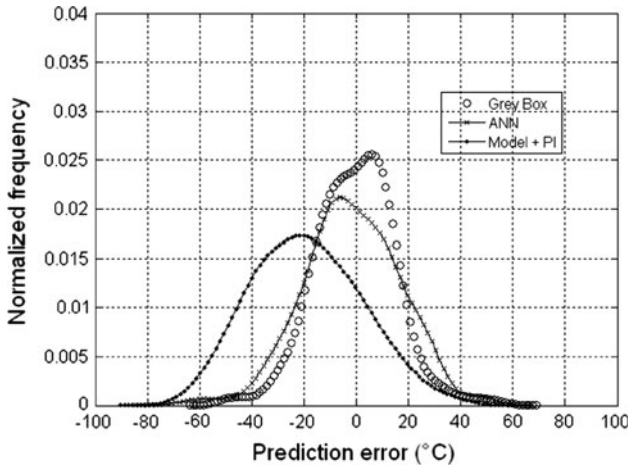

Fig. 12 Histogram of the estimation error of the model + PI, ANNs, and Gray-Box

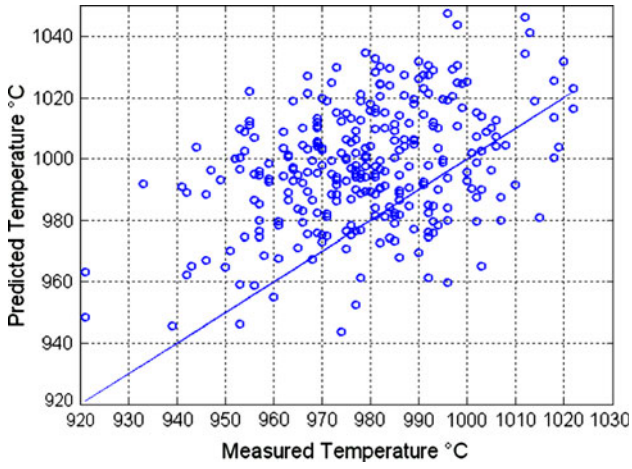

Fig. 13 Dispersion diagram of model + PI predicted SB entry temperature against measured SB entry temperature

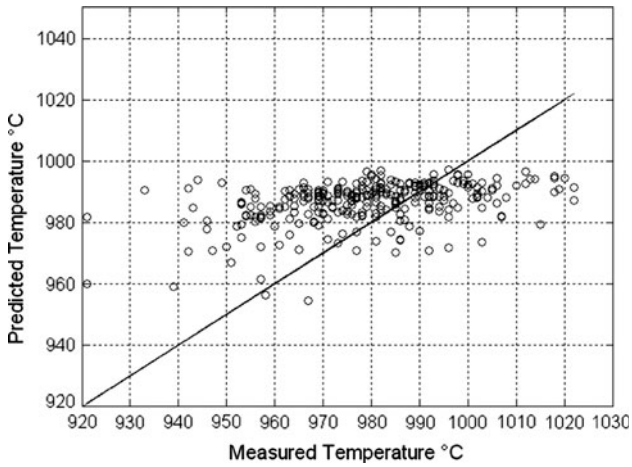

Fig. 14 Dispersion diagram of Gray-Box predicted SB entry temperature against measured SB entry temperature

7. Conclusions

In this article, one and two hidden layer ANNs and neural-based Gray-Boxes with 3, 5, or 7 neurons per layer were designed and applied for SB entry temperature estimation. Systems with some additional factors than those considered in the traditional physical modeling were also designed. The experiments were carried out using real information from plant. All neural systems developed here showed considerably better performance, and therefore better prediction capabilities, than the model + PI, with improvement ranging from 47 to 87% in bars with errors within 20 °C in some cases. However, Gray-Box schemes had slightly better performance than ANNs for the conditions tested here. The additional factors were also proven to have some influence on the heat loss process since they improved temperature prediction by about 10%. These results are promising, since by improving temperature prediction, the systems developed here may contribute to process throughput; however, in order for these systems to be recommended for implementation more exhaustive tests are required. Future research should include further study on the influence of the additional factors and comparison with fuzzy-based systems (Ref 26).

Acknowledgments

This study was partially supported by PROMEP and CONACYT. The authors would like to thank Dr. Jorge Ramirez from TERNIUM-Hylsa for providing the necessary data and the support.

References

1. W.L. Roberts, *Flat Processing of Steel*, Marcel Dekker Inc, New York, 1988
2. General Electric Models, Users Reference, Vol 1, Roanaoke, VA, 1993
3. G.M. Mendez, L. Leduc, R. Colas, A. Cavazos, and R. Soto, Modelling Recalescence After Stock Reduction During Hot Strip Rolling, *Ironmak. Steelmak.*, 2006, **33**, p 484–492
4. Y. Bissessur, E.B. Martin, A.J. Morris, and P. Kitson, Fault Detection in Hot Steel Rolling Using Neural Networks and Multivariate Statistics, *IEE Proc. Control Theory Appl.*, 2000, **147**, p 633–640
5. T. Watanabe, H. Narazaki, A. Kitamura, Y. Takahashi, and H. Hasegawa, A New Mill-setup System for Hot Strip Rolling Mill that Integrates a Process Model and Expertise, *IEEE International Conference on Computational Cybernetics and Simulation*, Vol 3, 1997, Orlando, FL, p 2818–2822
6. P. Maheral, K. Ide, T. Gomi, N. Pussegoda, and J.J.M. Too, Artificial Intelligence Technique in the Hot Rolling of Steel, *IEEE Canadian Conference on Electrical and Computer Engineering*, 1995, Montreal, Canada, p 507–510
7. D.A. Linkens, J.H. Beynon, and C.M. Sellars, Grey Box Modelling Methodologies and Their Application to Materials Processing, *Australasia Pacific Forum on Intelligent Processing and Manufacturing of Materials*, Vol 2, 1997, Gold Coast, Australia, p 676
8. N. Sato, N. Kamada, S. Naito, T. Fukushima, and M. Fujino, Application of Fuzzy Control System to Hot Strip Mill, *Proceedings of the IEEE International Conference on Industrial Electronics, Control, Instrumentation*, 1992, San Diego, CA, p 1202–1206
9. T. Martinetz, P. Protzel, O. Gramchow, and G. Sorgel, Neural Network Control for Rolling Mills, *EUFIT 94*, ELITE Foundation, Achen, Germany, 1994, p 147–152
10. M. Schalng and T. Poppe, Neural Network for Steel Manufacturing, *IEEE Expert*, 1996, **11**, p 8–9
11. X. Yao, A.K. Tieu, X.D. Fang, and D. Frances, Neural Network Application to Head & Tail Width Control in Hot Strip Mill, *IEEE International Conference on Neural Networks*, Vol 1, 1995, Orlando, FL, p 433–437
12. Y.S. Kim, B.J. Yum, and M. Kim, Robust Design of Artificial Neural Network for Roll Force Prediction in Hot Strip Mill, *IEEE International Joint Conference on Neural Network*, Vol 4, 2001, Washington, DC, p 2800–2804
13. G.M. Mendez, A. Cavazos, R. Soto, and L. Leduc, Entry Temperature Prediction of a Hot Strip Mill by a Hybrid Learning Type-2 FLS, *J. Intell. Fuzzy Syst.*, 2006, **17**(6), p 583–596
14. C. Min-You, Material Property Prediction Using Neural Fuzzy Network, *Proceedings of the IEEE, 3rd World Congress on Intelligent Control and Automation*, Vol 2, 2000, Hefei, China, p 1092
15. M. Mahfouf, M.A. Gama, and G. Panoutsos, Right-First-Time Production: A Reality or a Myth?, *Mater. Manuf. Process.*, 2009, **24**(1), p 78–82
16. J.S. Anderson, T.J. McAvoy, and O.J. Hao, Use of Hybrid Models in Wastewater Systems, *Ind. Eng. Chem. Res.*, 2000, **39**(6), p 1694–1704
17. P. Potocnik, I. Grabec, and M. Setinc, Neural Net Based Hybrid Modeling of the Methanol Synthesis Process, *Neural Process. Lett.*, 2001, **11**, p 219–228
18. P. Lauret, H. Boyer, and J.C. Gatina, Hybrid Modelling of the Sucrose Crystal Growth Rate, *Int. J. Model. Simul.*, 2001, **21**, p 23–29
19. P.E. Rooke and H. Wang, Applying Combined Neural Network and Physical Modelling to the Retention Process in Papermaking, *Appita J.*, 2002, **55**(4), p 281–286

20. Q. Zhu, M.F. Abbod, J. Talamantes-Silva, C.M. Sellars, D.A. Linkens, and J.H. Beynon, Hybrid Modelling of Aluminum-Magnesium Alloy During Thermomechanical Processing in Terms of Physically-Based Neuro-Fuzzy and Finite Element Models, *Acta Mater.*, 2003, **51**, p 5051–5062
21. P.D. Hodgson, L.X. Kong, and C.H.J. Davies, The Prediction of the Hot Strength in Steels with an Integrated Phenomenological and Artificial Neural Network Model, *J. Mater. Process. Technol.*, 1999, **87**, p 131–138
22. M. Schlang, B. Lang, T. Poppe, T. Runkler, and K. Inzierl, Current and Future Development in Neural Computation in Steel Processing, *Control Eng. Pract.*, 2001, **9**, p 975–986
23. W. Geerdes, M. Torres, M. Cabrera, and A. Cavazos, An Application of Physics-based and Artificial Neural Network-Based Hybrid Temperature Prediction Schemes in a Hot Strip Mill, *J. Manuf. Sci.*, 2008, **130**(1), p 014501–014505
24. R. Colás, Modelling Heat Transfer During Hot Rolling of Steel Strip, *Model. Simul. Mater. Sci. Eng.*, 1995, **3**, p 437–453
25. J.M. Zurada, *Introduction to Neural Systems*, PWS Publishing Company, Boston, MA, 1992
26. J.A. Barrios, A. Cavazos, L. Leduc, and J. Ramirez, Fuzzy and Fuzzy Grey-Box Modelling for Entry Temperature Prediction in a Hot Strip Mill, *Mater. Manuf. Process*. 2010, in press